

Kondo effect in the presence of van Hove singularities: A numerical renormalization group study

A. K. Zhuravlev* and V. Yu. Irkhin†

Institute of Metal Physics, 620990 Ekaterinburg, Russia

(Received 21 September 2011; revised manuscript received 22 November 2011; published 13 December 2011)

A numerical renormalization-group investigation of the one-center $t - t'$ Kondo problem is performed for the square lattice accounting for logarithmic Van Hove singularities (VHS) in the electron density of states near the Fermi level. The magnetic susceptibility, entropy, and specific heat are calculated. The temperature dependencies of the thermodynamic properties in the presence of VHS turn out to be nontrivial. When the distance Δ between VHS and the Fermi level decreases, the inverse logarithm of the corresponding Kondo temperature T_K demonstrates a crossover from the standard linear to square-root dependence on the s - d exchange coupling. The low-temperature behavior of the magnetic susceptibility and specific heat are investigated, and the Wilson ratio is obtained. For $\Delta \rightarrow 0$ the Fermi-liquid behavior is broken.

DOI: [10.1103/PhysRevB.84.245111](https://doi.org/10.1103/PhysRevB.84.245111)

PACS number(s): 75.30.Mb, 71.28.+d

I. INTRODUCTION

The Kondo effect is extensively studied starting from pioneering works by Kondo,¹ who explained the minimum of resistance in metallic alloys owing to resonance s - d scattering of conduction electrons by magnetic impurities. The solution of the Kondo problem²⁻⁴ is a very beautiful chapter in the history of modern theoretical physics.

The Kondo phenomenon is a key for explaining the behavior of heavy-fermion compounds and Kondo lattices,^{5,6} non-Fermi-liquid (NFL) systems,^{7,8} anomalous electronic properties of metallic glasses,⁹ quantum dots,¹⁰ and other systems. The Kondo anomalies are also studied in systems of reduced dimensionality, where they have a number of experimental peculiarities.¹¹ It is evident that the Kondo effect in such systems has a number of peculiar features from the theoretical point of view too.

The Kondo effect owing to Cu^{2+} spins in the CuO_2 planes is observed in layered n -type cuprates $(\text{La,Ce})_2\text{CuO}_4$, $(\text{Pr,Ce})_2\text{Cu}_4$, and $(\text{Nd,Ce})_2\text{CuO}_{4-\delta}$.¹²

Recently, the Kondo effect in graphene (a truly two-dimensional system with a peculiar electron spectrum) has been discussed.¹³⁻¹⁵ Because of the pseudogap in the spectrum, the Kondo effect for the undoped graphene exists under restricted conditions only, but for a doped substance the Kondo phase is present for all parameters.¹⁴

We can mention also some layered f systems where experimental investigations and first-principle band calculations demonstrate existence of two-dimensional features in electron properties. Examples are the compounds CeCoIn_5 (where the layers CeIn are present),¹⁶ CeCoGe_2 ,¹⁷ CePt_2In_7 ,¹⁸ CeRhIn_5 , Ce_2RhIn_8 ,¹⁹ and $\text{UCo}_{0.5}\text{Sb}_2$ (where two-dimensional weak localization is observed).²⁰

The layered Kondo lattice model was proposed for quantum critical beta YbAlB_4 , where two-dimensional boron layers are Kondo coupled via interlayer Yb moments.²¹ CeRuPO seems to be one of the rare examples of a ferromagnetic Kondo lattice where LSDA + U calculations evidence a quasi-two-dimensional electronic band structure, reflecting a strong covalent bonding within the CeO and RuP layers and a weak ionic-like bonding between the layers.²²

The above f systems demonstrate often both local-moment and itinerant-electron features. A large linear specific heat

coefficient and NFL behavior are observed also in some d systems, including layered ruthenates Sr_2RuO_4 ²³ and $\text{Sr}_3\text{Ru}_2\text{O}_7$.²⁴ Besides correlation effects, anomalies of electron properties in such systems are owing to the presence of Van Hove singularities (VHS) near the Fermi level.

In the present work we treat the one-center Kondo problem with the singular electron density of states. Earlier this problem was considered by Gogolin,²⁵ who used a “fast parquet” approach. In fact, such complicated methods are somewhat ambiguous, and the numerical renormalization-group (NRG) results of the paper²⁶ do not agree with the results of Ref. 25. Therefore we start in Sec. 2 from the standard perturbation theory and also apply the “poor man scaling” approach by Anderson.²⁷

In Sec. 3 we apply to the problem the NRG method, the technical details for our case being considered in the Appendix. The simple perturbation results for the Kondo temperature agree with NRG much better than the parquet results.²⁵ The physical quantities in the presence of the logarithmic singularity near the Fermi level are investigated. We calculate the magnetic susceptibility and specific heat, in particular at low temperatures, obtain the Wilson ratio, and discuss the problem of universal behavior.

II. THE KONDO MODEL WITH VAN HOVE SINGULARITIES

We use the Hamiltonian of the one-center s - d (f) exchange (Kondo) model:

$$H_{sd} = \sum_{\mathbf{k}\sigma} \varepsilon_{\mathbf{k}} c_{\mathbf{k}\sigma}^\dagger c_{\mathbf{k}\sigma} - \sum_{\mathbf{k}\mathbf{k}'\alpha\beta} J_{\mathbf{k}\mathbf{k}'} \mathbf{S} \sigma_{\alpha\beta} c_{\mathbf{k}\alpha}^\dagger c_{\mathbf{k}'\beta}. \quad (1)$$

Here $\varepsilon_{\mathbf{k}}$ is the band energy; \mathbf{S} are spin operators; σ are the Pauli matrices; in the case of contact coupling, $J_{\mathbf{k}\mathbf{k}'} = J/N_s$, where J is the s - d (f) exchange parameter; and N_s is the number of lattice sites.

Kondo¹ found that high-order perturbation contributions to various physical properties contain logarithmically divergent corrections. As demonstrated by further investigations of the Kondo problem, there occurs a pole at the boundary of the strong-coupling region, which is called the Kondo temperature

(in fact, this is a crossover scale). For a smooth density of states $\rho(E)$ this quantity is estimated as

$$T_K \propto D \exp \frac{1}{2J\rho(0)}, \quad (2)$$

where D is the half bandwidth. We treat the case of the logarithmically divergent bare density of electron states:

$$\rho(E) = A \ln \frac{D}{B|E + \Delta|}, \quad (3)$$

(the energy is referred to the Fermi level; the constants A , B , and Δ are determined by the band spectrum). The logarithmic divergence in $\rho(E)$ is typical for the two-dimensional case (in particular, for the layered ruthenates). However, similar strong Van Hove singularities can occur also in some three-dimensional systems, like Pd alloys and weak itinerant ferromagnets $ZrZn_2$ and $TiBr_2$.^{28,29}

First we consider the perturbation expansion for the resistivity, following the original approach by Kondo.¹ We write down the inverse transport relaxation time with the Kondo correction:

$$\tau^{-1}(E) = \tau_0^{-1}(E)[1 + 4Jg(E,0)], \quad (4)$$

Here,

$$g(E,T) = \sum_{\mathbf{k}} \frac{1/2 - n_{\mathbf{k}}}{E - \varepsilon_{\mathbf{k}}} = \int dE' \rho(E') \frac{1/2 - f(E')}{E - E'}, \quad (5)$$

with $n_{\mathbf{k}} = f(\varepsilon_{\mathbf{k}})$ being the Fermi function. After integration by part, in the case $\Delta = 0$ we obtain logarithmic accuracy for the resistivity:

$$R_{sd} \sim \int dE \rho(E) \left(-\frac{\partial f(E)}{\partial E} \right) \tau_0^{-1}(E) \times \left[1 - 2AJ \int dE' \left(-\frac{\partial f(E')}{\partial E'} \right) \ln^2 \left| \frac{D}{E'} \right| \right], \quad (6)$$

so that

$$R_{sd} = R_{sd}^{(0)} \left(1 - 2AJ \ln^2 \frac{D}{T} \right), \quad (7)$$

$$R_{sd}^{(0)} \sim J^2 S(S+1) A \ln \frac{D}{T}.$$

Applying the Abrikosov–Suhl summation (see Ref. 1), we have

$$R_{sd} = R_{sd}^{(0)} \left(1 + JA \ln^2 \frac{D}{T} \right)^{-2}, \quad (8)$$

which yields a nonstandard expression for the Kondo temperature:

$$T_K \simeq D \exp \left[- \left| \frac{1}{AJ} \right|^{1/2} \right]. \quad (9)$$

We calculate also the Kondo corrections to the static impurity magnetic susceptibility by generalizing a consideration of Ref. 1 to the case of the singular density of states. Expanding to second order in J , we derive (cf. Refs. 1,4, and 30)

$$\chi(T) = \frac{S(S+1)}{3T} \left[1 + 2J\chi^{(0)} - 2J^2 \sum_{\mathbf{k}\mathbf{k}'} \frac{n_{\mathbf{k}}(1-n_{\mathbf{k}'})}{(\varepsilon_{\mathbf{k}} - \varepsilon_{\mathbf{k}'})^2} \right], \quad (10)$$

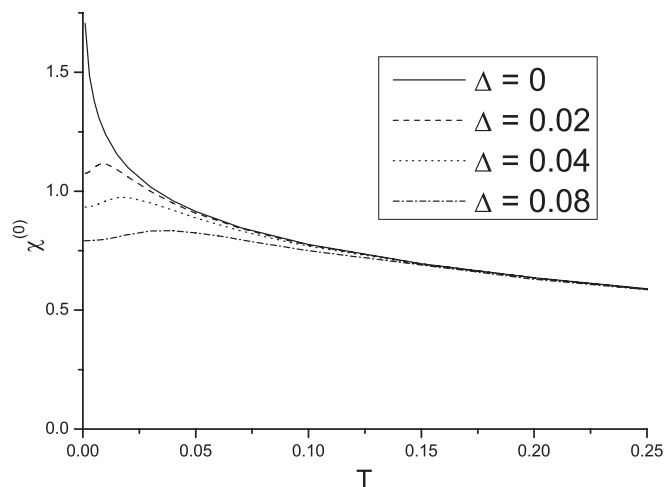


FIG. 1. The temperature dependence of noninteracting magnetic susceptibility for conduction electrons $\chi^{(0)}(T)$ at $\Delta = 0, 0.02, 0.04$, and 0.08 .

where

$$\chi^{(0)}(T) = - \sum_{\mathbf{k}} \frac{\partial n_{\mathbf{k}}}{\partial \varepsilon_{\mathbf{k}}} = \int dE \rho(E) \left[-\frac{\partial f(E)}{\partial E} \right] \simeq A \ln \frac{D}{\max(\Delta - T, T)} \quad (11)$$

is the Pauli susceptibility of noninteracting conduction electrons with the singular density of states, which is shown in Fig. 1. For $\Delta \neq 0$ this quantity has a maximum at $T \simeq \Delta/2$. Such a behavior is typical for the case where a density-of-states peak is present near the Fermi level.³¹

Performing integration and summation of the series of logarithmic terms, we have

$$\chi(T) = \frac{S(S+1)}{3T} \left[1 + \frac{2J\chi^{(0)}}{1 + J\chi^{(0)} \ln(D/T)} \right], \quad (12)$$

which yields at $\Delta = 0$ the same result for the Kondo temperature Eq. (9).

The correction to magnetic impurity entropy can be written down in an analogous way to obtain^{1,4}

$$S_{\text{imp}}(T) = \ln(2S+1) + \frac{\pi^2}{3} \frac{S(S+1)[2J\chi^{(0)}]^3}{[1 + J\chi^{(0)} \ln(D/T)]^3}. \quad (13)$$

Then we have, for impurity specific heat,

$$C_{\text{imp}}(T) = T \frac{dS_{\text{imp}}(T)}{dT} = \frac{\pi^2 S(S+1)}{[1 + J\chi^{(0)} \ln(D/T)]^4} \times \left\{ [2J\chi^{(0)}]^4 + 8J^3 T \frac{d\chi^{(0)}}{dT} [\chi^{(0)}]^2 \right\}. \quad (14)$$

The first term in the brackets yields the same structure as in the case of a smooth density of states [where $\chi^{(0)} = \rho$ and the singular contribution occurs in the fifth order in J only], and the second term is owing to logarithmic singularity in $\chi^{(0)}$. Being of the third order in J , the latter term can dominate. Additionally, it can change its sign and become negative; as we shall see below in Sec. III, this fact is important for the $C_{\text{imp}}(T)$ behavior.

Of course, the above expressions are applicable for $T > T_K$ only.

To perform a more formal consideration, we can apply the ‘‘poor man scaling’’ approach by Anderson.^{4,27} He progressively reduced the effective half bandwidth \tilde{D} of the conduction electrons and calculated perturbatively the effective interaction \tilde{J} renormalized due to the elimination of virtual excitations to the band edges. To carry out this scaling one divides the conduction band into states $|\varepsilon_{\mathbf{k}}| < \tilde{D} - |\delta\tilde{D}|$, which are retained, and states within the intervals $|\delta\tilde{D}|$ at the band edges, which are to be eliminated. In our model we obtain

$$\delta\tilde{J} = \tilde{J}[\rho(\tilde{D}) + \rho(-\tilde{D})] \frac{|\delta\tilde{D}|}{\tilde{D}}. \quad (15)$$

Then we derive the scaling equation:

$$\frac{\partial}{\partial |\tilde{D}|} \frac{1}{\tilde{J}} = -\frac{A}{\tilde{D}} \left(\ln \frac{D}{B|\tilde{D} + \Delta|} + \ln \frac{D}{B|-\tilde{D} + \Delta|} \right), \quad (16)$$

with the initial condition $\tilde{J}(D) = J$.

Solving this equation for $\Delta \rightarrow 0$ (as we shall see below, for $T_K \gg \Delta$), we derive

$$\frac{1}{\tilde{J}} = \frac{1}{J} + A \ln^2 \left| \frac{D}{B\tilde{D}} \right| - A \ln^2 \left| \frac{1}{B} \right|. \quad (17)$$

Then we obtain from the condition $1/\tilde{J}(T_K) = 0$ to the leading logarithmic approximation the result Eq. (9) again.

One can see that expression (9) is different from the corresponding parquet result:²⁵

$$T_K \simeq D \exp \left[- \left| \frac{2}{AJ} \right|^{1/2} \right]. \quad (18)$$

However, the NRG calculations²⁶ confirm the perturbation expression (9) rather than Eq. (18) (see the discussion below). The corresponding problems of the parquet approximation in the Hubbard model are treated in the works.³²

III. RESULTS OF NUMERICAL CALCULATIONS

We consider the $S = 1/2$ Kondo model for the square lattice with the band energy

$$\varepsilon_{\mathbf{k}} = 2t(\cos k_x + \cos k_y) + 4t'(\cos k_x \cos k_y - 1). \quad (19)$$

The spectrum Eq. (19) is shifted to restrict the band edges by $|E| < D = 4|t|$. The corresponding density of states is

$$\rho(E) = \frac{1}{2\pi^2 \sqrt{t^2 + Et' + 4t'^2}} K \left(\sqrt{\frac{t^2 - E^2/16}{t^2 + Et' + 4t'^2}} \right), \quad (20)$$

where $K(E)$ is the complete elliptic integral of the first kind.

For $t' = 0$ we have

$$\rho(E) = \frac{2}{\pi^2 D} K \left(\sqrt{1 - \frac{E^2}{D^2}} \right) \simeq \frac{2}{\pi^2 D} \ln \frac{4D}{|E|}, \quad (21)$$

so that, according to Eq. (9),

$$T_K \simeq D \exp \left[- \left| \frac{\pi^2 D}{2J} \right|^{1/2} \right]. \quad (22)$$

For nonzero t' the logarithmic Van Hove singularity is located at $E = -8t'$:

$$\rho(E) \simeq \frac{1}{2\pi^2 \sqrt{t^2 - 4t'^2}} \ln \frac{16\sqrt{t^2 - 4t'^2}}{|E + 8t'|}. \quad (23)$$

The distance Δ from the Van Hove singularity to the chemical potential μ is $\Delta = \mu + 8t'$. Thus the cutoff for the singular contributions is given by a single parameter Δ , which takes into account the shift of both the chemical potential and VHS from the band center. The NRG calculations performed demonstrated that for a fixed Δ the results depend very weakly on the concrete choice of t' and μ . The corresponding curves are visually indistinguishable (small deviations occur at high temperatures only). Therefore we present the results for $\mu = 0$ only.

The details of NRG calculations are discussed in the Appendix. When presenting numerical results in terms of Δ and J , we put $D = 1$.

The Kondo temperature in NRG calculations is determined from the temperature dependence of impurity magnetic susceptibility $\chi_{\text{imp}}(T)$ by using the condition $T_K \chi_{\text{imp}}(T_K) = 0.0701$ that is standard in the NRG method.²

Figures 2 and 3 show the dependence of the Kondo temperature on the bare coupling $|J|$ in the logarithmic scale. One can see that for finite Δ there occurs a crossover with decreasing $|J|$ from the square-root dependence Eq. (9) to the standard Kondo behavior Eq. (2). This crossover is qualitatively described by the lowest-order scaling.

It should be noted that the Kondo phenomenon should be invariant under the transformation $\varepsilon_{\mathbf{k}} \rightarrow -\varepsilon_{\mathbf{k}}$, i.e., $\rho(\varepsilon) \rightarrow \rho(-\varepsilon)$. However, the case of a nonsymmetric density of states using the formula $1 = 2Jg(T_K, 0)$ [where $g(E, T)$ is determined by Eq. (5)] yields slightly different results for the VHS peak above and below the Fermi level. Therefore we use the Nagaoka-Suhl formula (see Ref. 1):

$$1 = 2Jg(0, T_K), \quad (24)$$

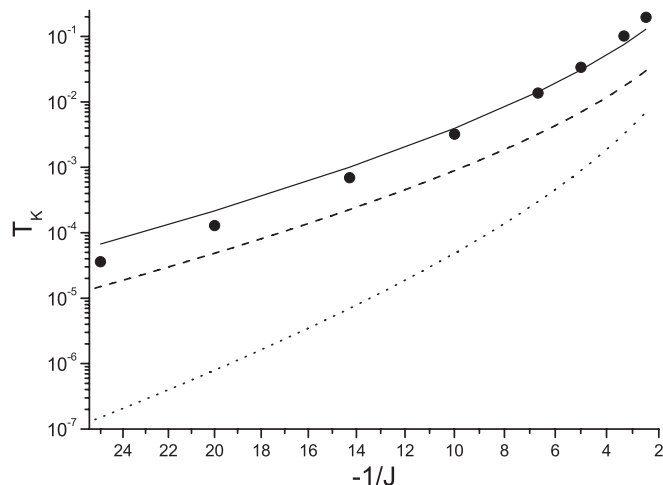


FIG. 2. The dependence $T_K(J)$ for $\Delta = 0$. Circles are NRG results, solid line corresponds to the Nagaoka-Suhl formula (24), dashed line corresponds to Eq. (22), and dotted line corresponds to Eq. (18) (without accounting for the pre-exponential multiplier).

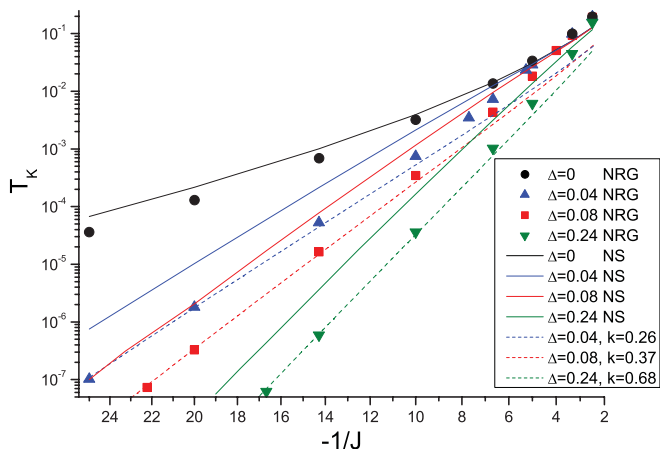


FIG. 3. (Color online) The dependencies $T_K(J)$ for $\Delta = 0, 0.04, 0.08,$ and 0.24 . Circles, top-up triangles, squares, and top-down triangles are the corresponding NRG results; solid lines (from above to below) correspond to the Nagaoka-Suhl (NS) formula (24); and dashed lines (from above to below) are results for small $|J|$ Eq. (25) with fitted constants k .

which works somewhat better at large $|J|$, but slightly worse at small $|J|$. (In fact, all such approximations yield nearly the same result at small $|J|$.)

According to Eq. (16), for $\Delta \ll T_K$ we have $\ln T_K \sim 1/\sqrt{|J|}$ and for $\Delta \gg T_K$ we come to the standard linear behavior $\ln T_K \sim 1/|J|$ with enhanced $\rho(0)$. For intermediate J , a crossover takes place.

The lowest-order scaling describes satisfactorily the numerical data at large $|J|$. However, it is insufficient to fit the numerical results at small $|J|$. Therefore we use the two-loop scaling result:^{2,4}

$$T_K = kD|2J\rho|^{1/2} \exp[1/2J\rho]. \quad (25)$$

This expression implies that only a small vicinity of the Fermi surface with nearly constant $\rho(E) \simeq \rho$ works. This assumption becomes not valid with increasing $|J|$, since the whole logarithmic peak becomes important. The fitting constant k should be determined by the whole form of the function $\rho(E)$. At small Δ , k is small since the quantity $\rho(0)$ is large owing to VHS peaks. On the contrary, for larger Δ (e.g., $\Delta = 0.24$), $\rho(0)$ becomes small.

Since T_K is high in our case of the singular density of states, the consideration of the situation with $\Delta \sim T_K$ is quite realistic. We can see that appreciable deviations from Eq. (25) owing to the singularity occur even for Δ being not too small and exceeding T_K .

The magnetic susceptibility owing to impurity spin can be expressed as a difference of magnetic susceptibilities of the whole system and the system without impurity:

$$\chi(T) \equiv \chi_{\text{imp}}(T) = \chi_{\text{tot}}(T) - \chi_{\text{band}}(T), \quad (26)$$

where χ_{tot} is the total magnetic susceptibility and $\chi_{\text{band}} = 2N_s\chi^{(0)}$ is the susceptibility of noninteracting band electrons (for two-spin projections). Apart from the susceptibility

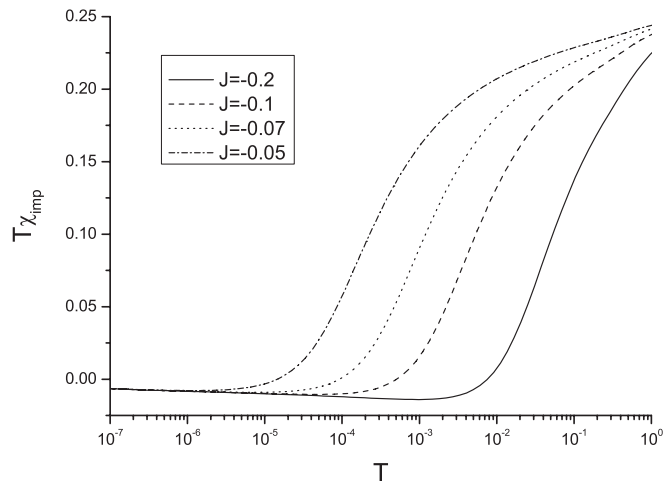


FIG. 4. The temperature dependence $T\chi_{\text{imp}}(T)$ for $\Delta = 0$ and $J = -0.2, -0.1, -0.07,$ and -0.05 (lines from below to above).

Eq. (26), the so-called local magnetic susceptibility χ_{loc} is frequently introduced as well:

$$\chi_{\text{loc}}(T) = \int_0^{1/T} \langle S_z(\tau)S_z \rangle d\tau. \quad (27)$$

This is the susceptibility of a *single* impurity in a magnetic field that acts locally only on this impurity; its magnitude, therefore, can hardly be measured experimentally, unlike χ_{imp} . In principle, χ_{imp} and χ_{loc} can behave quite differently. Such a possibility was mentioned in Ref. 33, where the reason for the difference is related to the energy dependence $\rho(E)$ and it is asserted that this difference disappears for a flat band of half width D in the limit of $D \rightarrow \infty$.

Figures 4–6 show the temperature dependence of magnetic susceptibility for different Δ values. $\chi(T)$ obeys the Curie law at high temperatures and demonstrates the Fermi-liquid behavior at low temperatures (except for the case $\Delta \rightarrow 0$).

For the standard flat-band case one has $T\chi(T) = \phi(T/T_K)$, so that the curves $T\chi(T)$ are universal: a change in J results in a change of T_K only. In our situation, such a simple universality

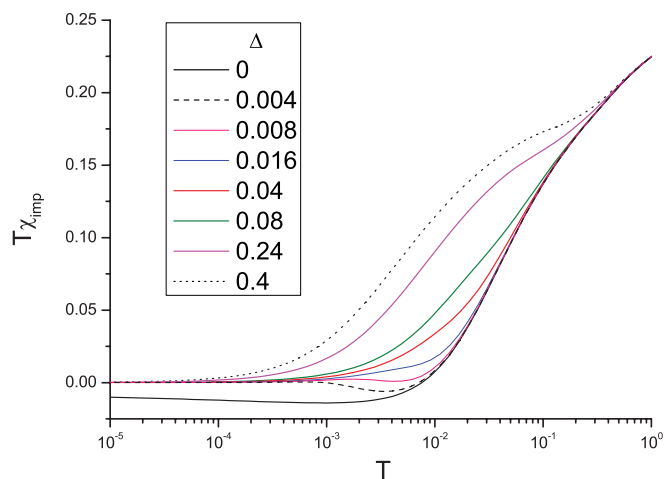


FIG. 5. (Color online) The temperature dependence $T\chi_{\text{imp}}(T)$ for $J = -0.2$ and $\Delta = 0, 0.004, 0.008, 0.016, 0.04, 0.08, 0.24,$ and 0.4 (lines from below to above).

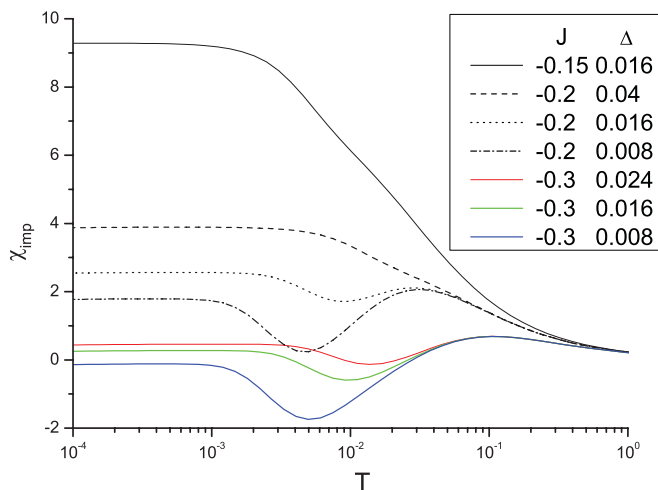


FIG. 6. (Color online) The temperature dependence $\chi_{\text{imp}}(T)$ for different J and Δ .

does not hold. In particular, for $\Delta = 0$ this fact (illustrated by Fig. 4) was demonstrated in Ref. 26.

One can see from Fig. 6 that a minimum in $\chi(T)$ occurs with decreasing Δ , its position being determined by the maximum of $\chi^{(0)}(T)$ in Eq. (11). This minimum is due to the strong energy dependence of the bare density of states; see Eqs. (10)–(12). Thus, besides the Kondo temperature T_K , a second characteristic scale can occur in our problem, which is determined by Δ . Therefore, we have to discuss the meaning of the Kondo temperature T_K in more detail. This quantity comes from the expansion in J starting from high temperatures where the impurity susceptibility $\chi(T)$ demonstrates the Curie behavior. T_K is determined as a temperature scale where a considerable deviation from this behavior occurs. In the flat-band situation and for smooth $\rho(E)$, $\chi(T)$ decreases monotonously with increasing T , the universal behavior taking place. This picture is characterized by the ratio $w = 4T_K\chi(0) \approx 0.41$,²⁻⁴ which relates high- and low-temperature scales T_K and $\chi(0)$. Such a behavior holds for $T_K < \Delta$, but for small Δ values the universality is broken, so that the intermediate-temperature dependence $\chi(T)$ becomes complicated and w deviates from 0.41 (see Table I).

The impurity entropy S_{imp} and specific heat C_{imp} are defined similarly to Eq. (26).

The Wilson ratio $R = (4\pi^2/3)\chi_{\text{imp}}(0)/\gamma_{\text{imp}}$ relating the low-temperature susceptibility and linear specific heat coefficient $\gamma_{\text{imp}} = C_{\text{imp}}/T$ is also presented in Table I. It is important that even for rather small Δ the value of R is still close to 2. Therefore a Fermi-liquid behavior, characteristic for the Kondo problem,² is restored at low temperatures, except for the case of extremely small Δ where $\chi_{\text{imp}}(0)$ and $C_{\text{imp}}(0)$ can even become negative.

Occurrence of negative values of χ_{imp} and S_{imp} was demonstrated in Ref. 26 by a strict analytical consideration of the simple case $J = -\infty$ for the semielliptic density of states. This is a common property of the Kondo model Eq. (1) with very narrow density-of-states peaks near the Fermi level. Of course, the quantities χ_{tot} and χ_{band} remain positive.

The singular case $\Delta \rightarrow 0$ demonstrates an essentially non-Fermi-liquid behavior (divergence of impurity magnetic

TABLE I. Results of our NRG calculations for different Δ and J : T_K (first line), Wilson ratio R (second line), and the quantity $w = 4T_K\chi(0)$ (third line; Wilson's value is $w = 0.4128 \pm 0.002$).

Δ	$J = -0.1$	$J = -0.15$	$J = -0.2$	$J = -0.3$
0.4	$1.19 \cdot 10^{-5}$ 2.008 0.414	$4.76 \cdot 10^{-4}$ 2.008 0.416	$3.33 \cdot 10^{-3}$ 2.014 0.416	0.0277 1.99 0.415
0.24	$3.62 \cdot 10^{-5}$ 1.995 0.413	$1.03 \cdot 10^{-3}$ 1.988 0.413	$6.13 \cdot 10^{-3}$ 2.005 0.414	0.0450 1.98 0.413
0.08	$3.45 \cdot 10^{-4}$ 1.998 0.415	$4.36 \cdot 10^{-3}$ 1.995 0.416	$1.84 \cdot 10^{-2}$ 1.991 0.425	0.0930 2.12 0.386
0.04	$7.49 \cdot 10^{-4}$ 1.999 0.416	$7.26 \cdot 10^{-3}$ 1.997 0.418	$2.88 \cdot 10^{-2}$ 2.069 0.447	0.0989 2.237 0.269
0.024	$1.12 \cdot 10^{-3}$ 2.002 0.417	$1.02 \cdot 10^{-2}$ 1.992 0.449	$3.20 \cdot 10^{-2}$ 1.998 0.392	0.1000 3.18 0.184
0.016	$1.44 \cdot 10^{-3}$ 1.996 0.417	$1.21 \cdot 10^{-2}$ 1.97 0.447	$3.30 \cdot 10^{-2}$ 2.040 0.337	0.1004 -177 ^a 0.108
0.008	$2.08 \cdot 10^{-3}$ 1.989 0.43	$1.34 \cdot 10^{-2}$ 2.03 0.38	$3.37 \cdot 10^{-2}$ 2.41 0.24	0.1006 0.343 ^a -0.048

^a $\chi(0) = 0.27$, $\gamma_{\text{imp}} = -0.02$

^a $\chi(0) = -0.12$, $\gamma_{\text{imp}} = -4.6$

susceptibility and specific heat at $T \rightarrow 0$). The low-temperature behavior at $\Delta = 0$ can be fit as²⁶

$$\chi_{\text{imp}} = -\frac{a}{T|\ln(T/D)|^\alpha}, \quad a \approx 0.072, \quad \alpha \approx 0.77, \quad (28)$$

$$S_{\text{imp}} = -\frac{b}{|\ln(T/D)|^\delta}, \quad b \approx 1.065, \quad \delta \approx 0.89, \quad (29)$$

(see Fig. 7), so that

$$C_{\text{imp}} = -\frac{b\delta}{|\ln(T/D)|^{\delta+1}}. \quad (30)$$

These asymptotics are independent of J (cf. Fig. 4), since at sufficiently low temperatures any value of $|J|$ manifold exceeds both the temperature and the width of the infinitely thin logarithmic peak in $\rho(E)$.

This situation is somewhat similar to the overscreened Kondo problem,³⁵ where the number of the scattering channels of conduction electrons $n > 2S$ (S is the localized spin value); in this case $\chi(T)$ demonstrates a power-law behavior, but remains positive.

As discussed in Ref. 36, a violation of the Fermi-liquid behavior with $C \propto 1/\ln^4(T_K/T)$ takes place in the case of the underscreened ($n < 2S$) Kondo problem.³⁶ This behavior of specific heat, as well as the correction to impurity magnetic susceptibility of the form $1/[T \ln(T_K/T)]$, occurs in the Bethe ansatz solution³ of the Kondo model too (as mentioned on page 621 of Ref. 3, such singularities can be also obtained from the solution of the Nagaoka equation starting from the

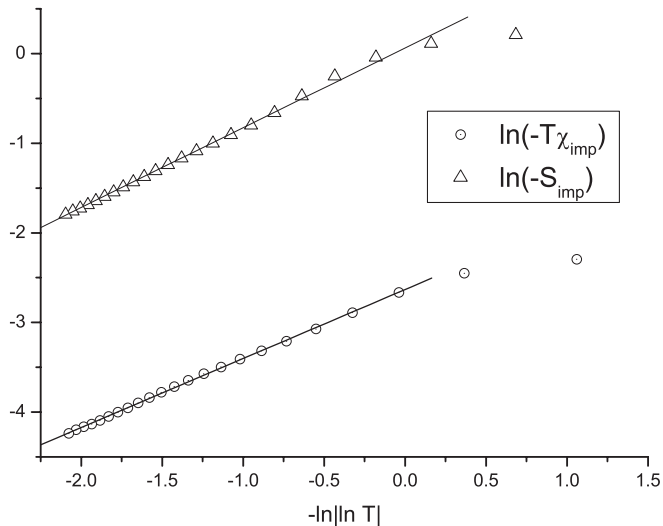


FIG. 7. The fitting of thermodynamic properties at low temperatures for $\Delta = 0$.

high-temperature perturbation expansion;¹ cf. equations of Sec. 2). It should be stressed that in this situation the magnetic moment remains positive ($S \rightarrow S - n/2$), and the singular contributions to thermodynamic properties have positive signs, unlike our case where such contributions are negative.

At the same time, in the standard Kondo screening situation [$n = 1$, $S = 1/2$, smooth $\rho(E)$] one has $T\chi(T) = O(T)$, so that the impurity moment is completely compensated by conduction electrons (note that $T\chi = \langle S_z^2 \rangle_{\text{tot}} - \langle S_z^2 \rangle_{\text{band}}$; see the Appendix). On the contrary, in the pseudogap situation (low density of states near μ , $\rho(E) \propto |E - \mu|^r$, $r > 0$), the screening is incomplete: $T\chi(T) > 0$.³⁴ In our case we have the opposite situation: $\rho(E \rightarrow 0)$ diverges and we have a (rather weak) overcompensation: $T\chi(T) < 0$. In other words, the Curie law is nearly fulfilled with a negative Curie constant, which tends very slowly to zero and remains appreciable at any reasonable low temperature (see Figs. 4–6).

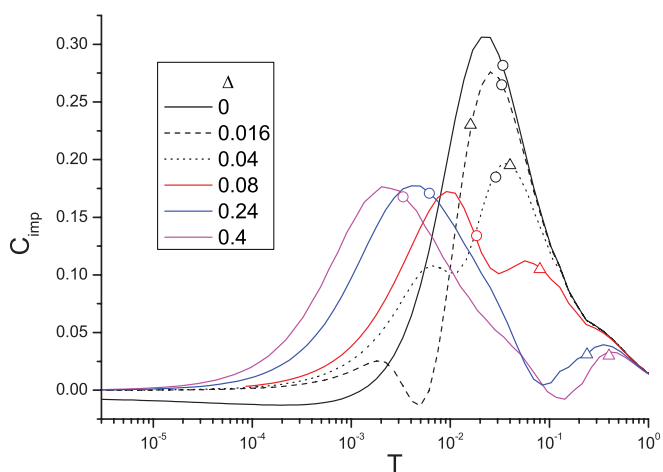


FIG. 8. (Color online) The temperature dependence of impurity specific heat for $J = -0.2$ and $\Delta = 0, 0.016, 0.04, 0.08, 0.24$, and 0.4 (lines from below to above, if one sees the left-hand part of the figure); circles mark T_K , and triangles mark Δ .

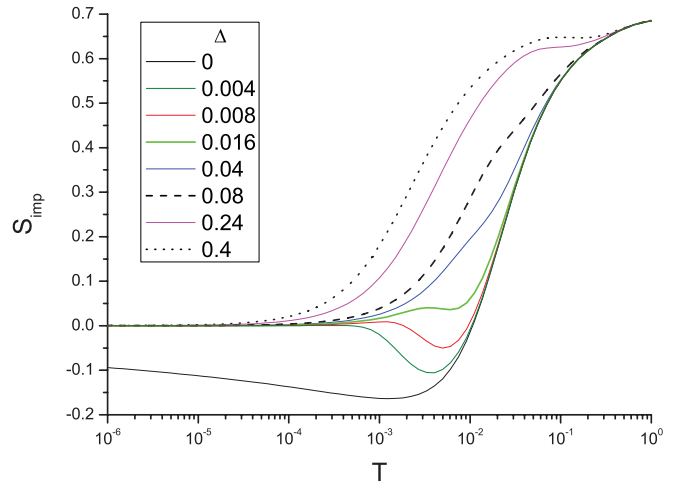


FIG. 9. (Color online) The temperature dependence of magnetic entropy for $J = -0.2$ and $\Delta = 0, 0.004, 0.008, 0.016, 0.04, 0.08, 0.24$, and 0.4 (lines from below to above).

Figure 8 shows the temperature dependence of impurity specific heat $C_{\text{imp}} = C_{\text{tot}} - C_{\text{band}}$ for different Δ . As a rule, this dependence demonstrates two peaks. At not too small Δ , the high-temperature maximum occurs at the temperature, determined by the distance from VHS to the chemical potential μ . This is owing to the nonmonotonous dependence of $\chi^{(0)}(T)$; see Eqs. (11) and (14). When decreasing temperature and passing this maximum, $C_{\text{imp}}(T)$ acquires a minimum and can even become negative. The low-temperature peak is owing to the Kondo effect and takes place in the standard flat-band situation too (see Ref. 38). One can see that its position corresponds roughly to the Kondo temperature. For small $\Delta < T_K$, the order of positions of the maxima becomes interchanged.

The corresponding magnetic entropy S_{imp} is shown in Fig. 9. One can see that this quantity tends to the value $\ln 2 = \ln(2S + 1)$ at high temperatures and demonstrates the Kondo compensation at low temperatures (except for overcompensation at $\Delta = 0$). The behavior turns out to be nonmonotonous due to the maximum in $\chi^{(0)}(T)$ [see Eq. (13)].

IV. CONCLUSIONS

The considered $t - t'$ Kondo problem is a nontrivial example of the influence of density-of-states peaks near the Fermi level on electron properties, which is combined with correlation effects (see a general discussion in Refs. 28 and 31). Our treatment gives an exact numerical solution of this problem. The overall picture obtained is rather rich, since this is governed by *two* key parameters: the Kondo temperature T_K (or the s - d coupling J) and the distance Δ between the Fermi level and VHS. The resulting temperature dependencies of thermodynamic properties include both one-particle effects connected with the Van Hove singularity and many-electron Kondo features and can be nonmonotonous. At low temperatures, as well as in the usual Kondo problem, the Fermi-liquid behavior is restored, except for the case of very small Δ . In the latter case, a non-Fermi-liquid behavior takes

place which should be studied in detail by more advanced analytical methods.

It would be also of interest to perform similar calculations for the Kondo lattice (heavy-fermion) problem, e.g., in some “mean-field” approximation. A “poor man scaling” approach was applied to this problem in Ref. 37.

ACKNOWLEDGMENTS

The research described was supported in part by the Programs “Quantum Physics of Condensed Matter” from the Presidium of Russian Academy of Sciences and “Strongly Correlated Electrons in Solids” from the Ural Branch of the Russian Academy of Sciences (12-T-2-1001). The authors are grateful to A. O. Anokhin and A. A. Katanin for useful discussions.

APPENDIX: NUMERICAL RENORMALIZATION-GROUP APPROACH FOR THE SINGULAR DENSITY OF STATES

Here, we discuss some important details of the numerical renormalization-group (NRG) method,^{2,39} as applied to our problem of the singular electron density of states.

1. Construction of the Wilson chain

Following Wilson,² we use a unitary transformation to pass from the operators $c_{\mathbf{k}}$ to the operators f_n . Then the impurity model with a Hamiltonian of the type Eq. (1) is reduced to a semi-infinite chain (Fig. 10) with a Hamiltonian of the type

$$H_{sd} = -J[S^+ f_{0\downarrow}^\dagger f_{0\uparrow} + S^- f_{0\uparrow}^\dagger f_{0\downarrow} + S_z(f_{0\uparrow}^\dagger f_{0\uparrow} - f_{0\downarrow}^\dagger f_{0\downarrow})] + \sum_{\sigma, n=0}^{\infty} [\epsilon_n f_{n\sigma}^\dagger f_{n\sigma} + \gamma_n(f_{n\sigma}^\dagger f_{n+1\sigma} + f_{n+1\sigma}^\dagger f_{n\sigma})]. \quad (\text{A1})$$

The renormalization-group procedure starts from the solution of the isolated-impurity problem (sites “imp” and ϵ_0 in Fig. 10). At the first step, we add a first conducting electronic site ϵ_1 and construct and diagonalize a Hamiltonian matrix on this Hilbert space (with a fourfold higher dimensionality). This procedure is multiple repeated. However, since the dimensionality of the Hilbert space grows as 4^N (N is the number of an iteration), it is impossible to store all the eigenstates during the calculation. Therefore, it is necessary to retain after each iteration only the states with the lowest energies. If we restrict ourselves to a certain maximum number of stored states (determined by the computational possibilities), it is necessary, starting from a certain iteration, to retain the order of one quarter of the states at each step.

Unfortunately, direct application of this scheme fails, since the disturbance introduced by the elimination of the high-lying

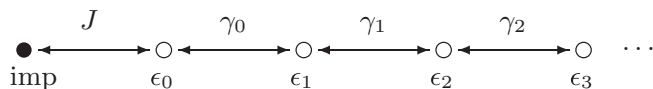


FIG. 10. Representation of the Kondo model in the form of a semi-infinite Wilson chain.

states turns out to be too large. Wilson found a method of overcoming this difficulty. This reduces to the artificial introduction of an exponential suppression of matrix elements γ_n , which decreases the coupling between the retained and eliminated states, thereby decreasing the influence of the eliminated states. To this end, Wilson² used a logarithmic discretization of the conduction band, i.e., replacement in Eq. (1) of an energy range $\epsilon_{\mathbf{k}} \in [\mu + \eta D \Lambda^{-m}, \mu + \eta D \Lambda^{-m+1}]$ ($\eta = 1, -1, m = 1, 2, 3, \dots$) by a single level with an energy $\bar{\epsilon}_{\eta m}$ equal to the average energy of this interval (D is the maximum of the distances between the chemical potential μ and two conduction band edges, $\Lambda > 1$). This results in a change of the density of states:

$$\rho(\epsilon) \rightarrow \sum_{\eta, m} \alpha_{\eta m}^2 \delta(\epsilon - \bar{\epsilon}_{\eta m}), \quad (\text{A2})$$

where

$$\alpha_{\eta m}^2 = \eta \int_{\mu + \eta D \Lambda^{-m}}^{\mu + \eta D \Lambda^{-m+1}} \rho(\epsilon) d\epsilon.$$

As a result, the jumps will have the required decay, $\gamma_n \propto \Lambda^{-n/2}$. For a flat band, Wilson obtained, analytically ($\mu = 0$),

$$\gamma_n = \frac{D(1 + \Lambda^{-1})(1 - \Lambda^{-n-1})}{2\sqrt{1 - \Lambda^{-2n-1}}\sqrt{1 - \Lambda^{-2n-3}}} \Lambda^{-n/2}, \quad \epsilon_n = 0. \quad (\text{A3})$$

In more complicated situations, the construction of the Wilson chain should be performed numerically. Usually (see, e.g., Ref. 40), this is performed in the spirit of the initial work,² by numerically reproducing Wilson’s analytical flat-band procedure for an arbitrary density of states. However, there exists another way which yields equivalent results, but seems to be more natural. To bring the matrix of Hamiltonian

$$H_\sigma = \sum_{\eta, m} \bar{\epsilon}_{\eta m} c_{\eta m, \sigma}^\dagger c_{\eta m, \sigma} \quad (\text{A4})$$

to the tridiagonal form, one can use the Lanczos tridiagonalization algorithm,⁴¹ which is adapted namely for this problem. For the model Eq. (1), this method was described in Ref. 4, where a Wilson chain for the nondiscretized semielliptic density of states was also analytically constructed. We perform this procedure numerically for an arbitrary logarithmically discretized density of states. Starting from the vector $|0\rangle = f_{0\sigma}^\dagger |\text{vac}\rangle$ (where $f_{0\sigma}^\dagger = \sum_{\eta, m} \alpha_{\eta m} c_{\eta m, \sigma}^\dagger$), we generate a new basis $|0\rangle, |1\rangle, |2\rangle, \dots$ for the conduction electron states by the Schmidt orthogonalization:

$$\begin{aligned} |1\rangle &= \frac{1}{\gamma_0} (H_\sigma |0\rangle - |0\rangle \langle 0| H_\sigma |0\rangle), \\ |2\rangle &= \frac{1}{\gamma_1} (H_\sigma |1\rangle - |1\rangle \langle 1| H_\sigma |1\rangle - |0\rangle \langle 0| H_\sigma |1\rangle), \\ |n+1\rangle &= \frac{1}{\gamma_n} (H_\sigma |n\rangle - |n\rangle \langle n| H_\sigma |n\rangle - |n-1\rangle \langle n-1| H_\sigma |n\rangle), \end{aligned} \quad (\text{A5})$$

where each γ_n is chosen to normalize $|n+1\rangle$. One can see that $\langle n'| H_\sigma |n\rangle = 0$ for $n' = 0, 1, 2, \dots, n-2$. This means that H_σ is tridiagonal in the new basis. The off-diagonal elements are $\langle n+1| H_\sigma |n\rangle = \gamma_n$. Defining $\epsilon_n \equiv \langle n| H_\sigma |n\rangle$, we consecutively obtain the coefficients γ_n and ϵ_n for Eq. (A1).

2. Calculation of thermodynamical averages

In our calculations, we put $\Lambda = 1.5$ and store 1×10^4 states per iteration.

Diagonalizing the Hamiltonian Eq. (A1) for a given chain length N yields a set of eigenvalues. As indicated in Ref. 2, because of retaining only part of the energy spectrum at the N th step of the NRG procedure, thermodynamic averages should be calculated at a temperature that depends on Λ , $T_N = \Lambda^{-N/2} T_0$, where the starting temperature T_0 is chosen more or less arbitrarily. However, it should be neither too large (then contributions of eliminated high-energy states become important), nor too small (then the discreteness of the energy spectrum become appreciable).

The total entropy and specific heat read³⁹

$$\begin{aligned} S_{\text{tot}} &= \langle H \rangle_{\text{tot}} / T + \ln Z_{\text{tot}}, \\ C_{\text{tot}} &= [\langle H^2 \rangle_{\text{tot}} - \langle H \rangle_{\text{tot}}^2] / T^2, \end{aligned} \quad (\text{A6})$$

where Z is partition function. Since the total spin commutes with the Hamiltonian H , each eigenvalue is characterized by a well-defined spin projection $S_{z,\text{tot}}$; therefore, the quantities like $\langle S_z^2 \rangle_{\text{tot}}$ can be calculated straightforwardly. On differentiating $\langle S_z \rangle_{\text{tot}}$ with respect to the magnetic field, one obtains²

$$T \chi_{\text{tot}}(T) = \langle S_z^2 \rangle_{\text{tot}} - \langle S_z \rangle_{\text{tot}}^2. \quad (\text{A7})$$

The quantities $T \chi_{\text{band}}(T)$, S_{band} , and C_{band} are calculated in a similar way, and the corresponding impurity contributions are obtained by subtracting them from Eqs. (A6) and (A7).

Because of the finite length of the chain, the thermodynamic quantities like $T_N \chi_{\text{imp}}(T_N)$ and $C_{\text{imp}}(T_N)$ demonstrate

even-odd oscillations depending on T_N , which have nearly constant amplitudes. Therefore, the amplitudes of the oscillations in $\chi_{\text{imp}}(T)$ and $C_{\text{imp}}(T)/T = \gamma_{\text{imp}}(T)$ increase strongly with lowering T .

To suppress the oscillations in $\chi_{\text{imp}}(T)$, we used smoothing according to Euler.⁴² For a certain oscillating sequence A_n we introduce a new sequence $A_n^{(1)}$ whose members are equal to averages of the adjacent members of the initial sequence: $A_n^{(1)} = (A_n + A_{n+1})/2$. If necessary, the procedure is repeated: $A_n^{(2)} = (A_n^{(1)} + A_{n+1}^{(1)})/2$. In particular, this was performed in the calculation of χ_{imp} . By designating $\chi_N \equiv \chi_{\text{imp}}(T_N)$, we obtain

$$\begin{aligned} \chi^{(1)}(\sqrt{T_N T_{N+1}}) &= \frac{1}{2} \chi_N + \frac{1}{2} \chi_{N+1}, \\ \chi^{(2)}(T_N) &= \frac{1}{4} \chi_{N-1} + \frac{1}{2} \chi_N + \frac{1}{4} \chi_{N+1}, \\ \chi^{(3)}(\sqrt{T_N T_{N+1}}) &= \frac{1}{8} \chi_{N-1} + \frac{3}{8} \chi_N + \frac{3}{8} \chi_{N+1} + \frac{1}{8} \chi_{N+2}. \end{aligned} \quad (\text{A8})$$

A similar problem, which occurs calculating the slope of specific heat γ_{imp} , is solved in the same way. The method was tested for the flat-band case to obtain the values $R = 2.008, 2.016$ and $w = 0.416, 0.417$ for $J = -0.1, -0.2$, respectively (cf. Table I). Our method differs from Ref. 2 by the fact that we calculate χ_{imp} and γ_{imp} directly rather than by explicitly constructing an effective Hamiltonian near the fixed point $J = -\infty$. Although resulting in a slight decrease of accuracy, such an approach can be applied more widely, in particular to obtain a NFL behavior (see Figs. 4–6).

*zhuravlev@imp.uran.ru

†valentin.irkhin@imp.uran.ru.

¹J. Kondo, in *Solid State Physics*, edited by F. Seitz, D. Turnbull, and H. Ehrenreich (Academic Press, New York, 1969), Vol. 23, p. 183.

²K. G. Wilson, *Rev. Mod. Phys.* **47**, 773 (1975); H. R. Krishna-Murthy, J. W. Wilkins, and K. G. Wilson, *Phys. Rev. B* **21**, 1003 (1980).

³A. M. Tsvelick and P. B. Wiegmann, *Adv. Phys.* **32**, 453 (1983).

⁴A. C. Hewson, *The Kondo Problem to Heavy Fermions* (Cambridge University Press, Cambridge, 1993).

⁵G. R. Stewart, *Rev. Mod. Phys.* **56**, 755 (1987).

⁶N. B. Brandt and V. V. Moshchalkov, *Adv. Phys.* **33**, 373 (1984).

⁷M. B. Maple *et al.*, *J. Low Temp. Phys.* **95**, 225 (1994); **99**, 223 (1995).

⁸G. R. Stewart, *Rev. Mod. Phys.* **73**, 797 (2001); **78**, 743 (2006).

⁹D. L. Cox and A. Zawadowski, *Adv. Phys.* **47**, 599 (1998).

¹⁰I. L. Aleiner, P. W. Brouwer, and L. I. Glazman, *Phys. Rep.* **358**, 309 (2002).

¹¹M. A. Blachly and N. Giordano, *Phys. Rev. B* **51**, 12537 (1995).

¹²J. L. Peng, R. N. Shelton, and H. B. Radousky, *Phys. Rev. B* **41**, 187 (1990); T. Sekitani, M. Naito, and N. Miura, *ibid.* **67**, 174503 (2003).

¹³K. Sengupta and G. Baskaran, *Phys. Rev. B* **77**, 045417 (2008).

¹⁴H. B. Zhuang, Q. Sun, and X. C. Xie, *Europhys. Lett.* **86**, 58004 (2009).

¹⁵T. O. Wehling, A. V. Balatsky, M. I. Katsnelson, A. I. Lichtenstein, and A. Rosch, *Phys. Rev. B* **81**, 115427 (2010).

¹⁶J. Costa-Quintana and F. Lopez-Aguilar, *Phys. Rev. B* **67**, 132507 (2003); A. Koitzsch *et al.*, *ibid.* **79**, 075104 (2009).

¹⁷C. R. Rotundu and B. Andracka, *Phys. Rev. B* **74**, 224423 (2006).

¹⁸M. Matsumoto, M. J. Han, J. Otsuki, and S. Yu. Savrasov, *Phys. Rev. B* **82**, 180515(R) (2010); N. apRoberts-Warren, A. P. Dioguardi, A. C. Shockley, C. H. Lin, J. Crocker, P. Klavins, and N. J. Curro, *ibid.* **81**, 180403 (2010).

¹⁹A. L. Cornelius, P. G. Pagliuso, M. F. Hundley, and J. L. Sarrao, *Phys. Rev. B* **64**, 144411 (2001); P. G. Pagliuso *et al.*, *ibid.* **66**, 054433 (2002).

²⁰V. H. Tran, R. Troc, Z. Bukowski, D. Badurski, and C. Sulkowski, *Phys. Rev. B* **71**, 094428 (2005).

²¹A. H. Nevidomskyy and P. Coleman, *Phys. Rev. Lett.* **102**, 077202 (2009).

²²C. Krellner, N. S. Kini, E. M. Bruning, K. Koch, H. Rosner, M. Nicklas, M. Baenitz, and C. Geibel, *Phys. Rev. B* **76**, 104418 (2007).

²³N. Kikugawa, C. Bergemann, A. P. Mackenzie, and Y. Maeno, *Phys. Rev. B* **70**, 134520 (2004).

²⁴S. I. Ikeda, Y. Maeno, S. Nakatsuji, M. Kosaka, and Y. Uwatoko, *Phys. Rev. B* **62**, R6089 (2000); A. Tamai *et al.*, *Phys. Rev. Lett.* **101**, 026407 (2008).

²⁵A. O. Gogolin, *Z. Phys. B* **92**, 55 (1993).

²⁶A. K. Zhuravlev, *Phys. Met. Metallogr.* **108**, 107 (2009).

²⁷P. W. Anderson, *J. Phys. C* **3**, 2436 (1970).

- ²⁸S. V. Vonsovskii, M. I. Katsnelson, and A. V. Trefilov, *Phys. Met. Metallogr.* **76**, 247 (1993).
- ²⁹T. Jeong, A. Kyker, and W. E. Pickett, *Phys. Rev. B* **73**, 115106 (2006).
- ³⁰V. Yu. Irkhin and M. I. Katsnelson, *Fiz. Tverd. Tela* **30**, 2273 (1988); *Z. Phys. B* **75**, 67 (1989).
- ³¹V. Yu. Irkhin and Yu. P. Irkhin, *Electronic Structure, Correlation Effects and Properties of d- and f-Metals and Their Compounds* (Cambridge International Science Publishing, Cambridge, 2007).
- ³²I. E. Dzyaloshinskii and V. M. Yakovenko, *Sov. Phys. JETP* **67**, 844 (1988); A. T. Zheleznyak, V. M. Yakovenko, and I. E. Dzyaloshinskii, *Phys. Rev. B* **55**, 3200 (1997).
- ³³G. E. Santoro and G. F. Giuliani, *Phys. Rev. B* **44**, 2209 (1991).
- ³⁴K. Ingersent, *Phys. Rev. B* **54**, 11936 (1996).
- ³⁵P. Coleman, L. B. Ioffe, and A. M. Tsvelik, *Phys. Rev. B* **52**, 6611 (1995).
- ³⁶P. Coleman and C. Pepin, *Phys. Rev. B* **68**, 220405(R) (2003).
- ³⁷V. Yu. Irkhin, *J. Phys. Condens. Matter* **23**, 065602 (2011).
- ³⁸L. N. Oliveira and J. W. Wilkins, *Phys. Rev. Lett.* **47**, 1553 (1981).
- ³⁹R. Bulla, T. A. Costi, and T. Pruschke, *Rev. Mod. Phys.* **80**, 395 (2008).
- ⁴⁰K. Chen and C. Jayaprakash, *Phys. Rev. B* **52**, 14436 (1995).
- ⁴¹B. N. Parlett, *The Symmetric Eigenvalue Problem* (Prentice-Hall, Englewood Cliffs, 1980).
- ⁴²G. H. Hardy, *Divergent Series* (American Mathematical Society, Chelsea, 1992).